TECHNICAL MATERIAL

Typeset with jnst.cls <ver.2.1>

Nuclear data sensitivity analysis on LWR nuclear fuel depletion with the modern evaluated nuclear data files

Hidayati Amar[1], Yuya Inagaki[2], Junshuang Fan[2], Tatsuya Fujita[2], Go Chiba[2]*

[1]*Nuclear Energy Regulatory Agency of Indonesia, Jakarta 10120, Indonesia ;*

[2]*Hokkaido University, Kita-ku, Sapporo 060-8628, Japan*

Nuclear data sensitivity analysis on light water reactor (LWR) nuclear fuel depletion with the modern evaluated nuclear data files were carried out. Sensitivity coefficients of the neutron multiplication factors k during nuclear fuel depletion to nuclear data were calculated using the reactor physics code system CBZ with the depletion perturbation theory. The single fuel pincell problems with UO_2 and MOX fuels, the 3×3 multicell problems, and the PWR fuel assembly problems were prepared. The six modern evaluated nuclear data files were used, and differences in k from the reference JENDL-4.0 results were discussed using the sensitivity coefficients. In the results of the single pincell problems, the UO_2 and MOX fuel problems show the different trend in the k_∞ differences. Ragarding the 3×3 multicell problems, the existance of gadolinium changes the trend of the k_∞ difference comparing with the single pincell model. The PWR assembly problems show the similar trend in the k_∞ difference as the 3×3 multicell problems.

Keywords: nuclear data, light water reactors, nuclear fuel depletion, sensitivity analysis

*Corresponding author. Email: go_chiba@eng.hokudai.ac.jp

1. Introduction

Nuclear data are crucial to quantify the neutronics properties of nuclear systems, and the evaluated nuclear data files (or libraries) are generally used. The evaluated nuclear data files have been developed by several countries/districts or organizations, and ENDF/B, JEFF, and JENDL are frequently referred. Those files have been updated once per several (or around ten) years based on newly accumulated differential/integral data and newly developed models on the nuclear physics. As in January of 2025, the latest versions of ENDF/B, JEFF, and JENDL are ENDF/B-VIII.1, JEFF-3.3[1], and JENDL-5[2], respectively. Although a lot of revisions have been made in these nuclear data files for the past years, there still be large differences in the evaluated nuclear data among these files. Some of the previous revisions had difficulty to be accepted in users' community for specific applications since the improvement could not be expected after the revisions.

In order to improve the quality of the evaluated nuclear data files, feedback from users community are beneficial. When neutronics parameters of nuclear systems (or integral parameters) are calculated with several different nuclear data files, differences among them generally arise. If these differences are significant, investigation on the origin of these differences is quite useful for the future nuclear data evaluations. In such cases, nuclear data users can perform two calculations where one is done with the first nuclear data file and the other is done after replacing specific nuclear data of the first file by that of the second file. If they can fortunately find the large difference in the calculated neutronics parameters, the origin of the difference can be identified. This kind of investigation, however, is cumbersome especially if detailed information such as type of the reaction and the concerned energy range are required. To do this, sensitivity coefficients (or the first-order derivatives of the neutronics parameters with respect to the nuclear data) are powerful since the origin of the difference in the neutronics parameters due to the differences in the nuclear data can be easily identified by using them. The usefulness of this procedure has

been well recognized in the field of nuclear reactor physics, and there have been several works based on that so far[5–7].

Sensitivity coefficients of the static neutronics parameters can be easily calculated with the classical or generalized perturbation theory. In addition, sensitivity coefficients of the parameters relevant with the nuclear fuel depletion can also be calculated with the depletion perturbation theory (DPT)[8,9]. Whereas DPT has been well established, examples of the actual implementations are limited. The reactor physics code system CBZ being developed at Hokkaido University has the DPT capability with which the sensitivity coefficients of the neutron multiplication factors and nuclide number densities during nuclear fuel depletion can be calculated for light water reactor (LWR) fuel assembly models[10]. In the present work, through sensitivity analysis on the neutron multiplication factor during fuel depletion of LWR using the DPT capability of CBZ, we attempt to draw the useful information which can be feedback to the community of nuclear data. In this work, only the reaction cross sections are concerned, and the modern general-purpose evaluated nuclear data files such as JENDL-4.0[11], -5, ENDF/B-VII.1, -VIII.0, -VIII.1, JEFF-3.2 and -3.3 are treated. The common data for the nuclide decay-relevant parameters and the fission product yields are used.

The present paper is organized as follows; Section 2 describes the theory of the nuclear data sensitivity analysis, and employed numerical methods and data; Section 3 is devoted to provide the problem specifications, and numerical results are presented in Section 4; Section 5 gives the conclusion of the present work.

2. Theory, numerical methods, and numerical data

2.1. Nuclear data sensitivity analysis

The neutron multiplication factor k of nuclear systems can be quantified by solving the neutron transport equation numerically. Since the neutron transport equation uses

the reaction cross sections defined from the evaluated nuclear data files, a change in the nuclear data will cause a change in k calculated from the transport equation. The sensitivity coefficient is introduced as an index to quantify the impact of change in each nuclear data on the k calculation, and is defined as

$$S = \frac{\partial k}{\partial \sigma} \cdot \frac{\sigma}{k}, \tag{1}$$

where σ is nuclear data and S is the sensitivity coefficient of k to σ.

Here two nuclear data files are considered and the nuclear data defined in each file is denoted to as σ^A and σ^B. The k calculation that uses these nuclear data files will give two results, k^A and k^B. The difference between k^A and k^B, Δk, can be estimated from the following equation:

$$\Delta k = k^A - k^B \approx \left(\frac{\partial k}{\partial \sigma}\right)\left(\sigma^A - \sigma^B\right). \tag{2}$$

The relative difference in k, $\Delta k/k^B$, can be written as follow:

$$\frac{\Delta k}{k^B} = \frac{k^A - k^B}{k^B} \approx \left(\frac{\partial k^B}{\partial \sigma^B} \cdot \frac{\sigma^B}{k^B}\right)\frac{\sigma^A - \sigma^B}{\sigma^B} = S^B \cdot \frac{\sigma^A - \sigma^B}{\sigma^B}. \tag{3}$$

As shown in this equation, the relative difference in k can be obtained by the product of the sensitivity coefficient and the relative difference in σ. If k^B is known and the sensitivity coefficient is available, we can estimate k^A with Equation (3) without solving the neutron transport equation defined from σ^A.

It should be reminded that Equation (2) is just an approximation, and the complete equation is written as follows:

$$\Delta k = \left(\frac{\partial k}{\partial \sigma}\right)\Delta\sigma + \frac{1}{2}\left(\frac{\partial^2 k}{\partial \sigma^2}\right)(\Delta\sigma)^2 + \frac{1}{3!}\left(\frac{\partial^3 k}{\partial \sigma^3}\right)(\Delta\sigma)^3 + \cdots. \tag{4}$$

If $\Delta\sigma$ is small, the effect of the terms above the second order is considered negligible, but otherwise these will also have an effect.

The nuclear data are defined for the nuclide, the type of reaction, and the neutron energy. In the framework of the deterministic calculation procedure, the neutron energy

is discretized into the energy groups. If we write the nuclear data for nuclide n, reaction x, and energy group g as $\sigma_{n,x,g}$ and write a sensitivity coefficient to $\sigma_{n,x,g}$ as $S_{n,x,g}$, Equation (3) can be written as follows:

$$\frac{k^A - k^B}{k^B} \approx \sum_n \sum_x \sum_g \left(S^B_{n,x,g} \cdot \frac{\sigma^A_{n,x,g} - \sigma^B_{n,x,g}}{\sigma^B_{n,x,g}} \right) = \sum_n \sum_x \sum_g \left(\frac{\Delta k}{k} \right)_{n,x,g}, \tag{5}$$

where $(\Delta k/k)_{n,x,g}$ is the relative difference in k resulting from the difference in the nuclear data of nuclide n, reaction type x, and energy group g.

There are several methods to calculate the sensitivity coefficient of the neutron multiplication factor to nuclear data. The simplest one is to slightly vary the nuclear data of interest and observe the corresponding variation in k. This can be expressed in the following equation:

$$\frac{\partial k}{\partial \sigma_i} = \frac{\Delta k}{\Delta \sigma_i} = \frac{k' - k}{\Delta \sigma_i}, \tag{6}$$

where k' denotes the multiplication factor obtained when the variation $\Delta\sigma_i$ is given to nuclear data σ_i. In principle, the sensitivity coefficient to any nuclear data can be calculated in this way, but we need to keep in mind that the nuclear data depend on nuclides, reactions, and energy groups. If the numbers of nuclides, reactions, and energy groups to be treated are N, X, and G, then the number of sensitivity coefficients to be calculated is $N \times X \times G$. To calculate sensitivity coefficients for all these nuclear data, k' calculations must be performed many times, and it requires a long computation time. On the other hand, there is an efficient method to calculate the sensitivity coefficients using the solution of the adjoint neutron transport equation based on the perturbation theory. In the first-order perturbation theory, the reactivity (or change in k) due to a perturbation of a system can be easily obtained from the forward and adjoint neutron fluxes of the system before the perturbation. Sensitivity coefficients can be calculated from the variation of k with the variation of cross section as shown in Equation (6), so the variation of cross section is regarded as a perturbation and the reactivity due to the perturbation can be

calculated based on the perturbation theory.

When neutronics parameters such as the neutron multiplication factor during the fuel depletion is concerned, two components must be taken into account in the impact of the cross section perturbation on the parameters. The first one is the direct component in which the cross section perturbation affects the transport equation at the concerned burnup state via microscopic cross sections. In addition to this direct component, the impact of the cross section perturbation on the nuclide number densities at the concerned burnup state should be considered since the cross section perturbation affects the nuclide transmutation during the fuel depletion until the concerned burnup state. This effect is known as the indirect (or burnup) component. The sensitivity coefficients including these two components can be calculated with DPT.

2.2. Numerical methods and data

In the present work, nuclear fuel depletion calculations were carried out with the reactor physics code system CBZ.

361-group libraries, whose energy group structure is taken from SHEM-361[12], were generated using the FRENDY code[13] from the evaluated nuclear data files. Only in the ENDF/B-VIII.1 processing, NJOY2016[14] was used for several nuclides including Pu-239. The effective (energy-averaged) 361-group cross sections were calculated with the advanced Bondarenko model[15] based on the background cross sections considering the lattice heterogeneity. The Dancoff factors were evaluated with the neutron current method[16]. The elastic scattering cross sections of H-1 below 4 eV were calculated from the thermal scattering law data for H-1 bounded in light water. The 361-group neutron transport equation defined from these effective cross sections was solved by the method of characteristics, and the neutron multiplication factor and the neutron flux were obtained at each burnup point. The scattering anisotropy was taken into account by the P0 transport ap-

proximation. The Bateman equation defined from the reaction rates based on the effective cross sections and the neutron flux obtained above was solved by the mini-max polynomial approximation[17,18], and nuclide number densities at the next burnup point were calculated. If the target systems contain burnable absorbers, the advanced optimally-weighted predictor-corrector method[19] was employed to reduce the time discretization error. This procedure was iteratively carried out until the fuel burnup becomes the specific value. The nuclide number density change was simulated with the nuclide transmutation chain consisting of 21 heavy nuclides and 138 fission products[20]. The decay data and fission yield data were taken from JENDL/FPD-2011 and JENDL/FPY-2011[21]. The overall procedure for the nuclear fuel depletion calculations with CBZ have been verified in our previous work[10].

In the current implementation of CBZ, the indirect component in the sensitivities for the (n,f), (n,γ), and (n,2n) cross sections of the nuclides included in the fuel pellet region and the (n,n) cross section of H-1 in the coolant can be calculated. Since the sensitivity coefficient calculation with DPT requires a huge amount of computer memory and long computation time, this calculation was carried out with the 107-group cross sections. The energy group structure was taken from that used in the SRAC code[22]. The upper and lower energy boundaries in the SHEM 361-group structure and the SRAC 107-group structure are different from each other: 19.6 MeV and 0.00011 eV in the former and 10 MeV and 0.00001 eV in the latter. The impact of this difference on the sensitivity analyses results is considered insignificant. In the sensitivity calculations, the weighted predictor-corrector method was employed for the systems containing burnable absorbers.

In the present work, 107-group sensitivity coefficients were calculated with JENDL-4.0-based library, and the cross section difference in the sensitivity analyses with Eq. (5) was calculated as differences from the JENDL-4.0 evaluation. While CBZ calculates sensitivity coefficients to the effective cross sections, the infinite dilution cross sections were used in

calculating the cross section difference in Eq. (5). This inconsistency might cause some errors in Δk.

3. Problem specification

3.1. Single pincell problems

PWR-simulated single fuel pincell problems consisting of fuel pellet, cladding, and coolant was prepared. Regarding the fuel compositions, three UO_2 fuels with U-235 enrichment of 3.4 wt%, 4.1 wt%, and 4.7 wt% and one MOX fuel with the plutonium content of 10 wt% were prepared. The transuranic composition of the MOX fuel is Pu-238/-239/-240/-241/-242/Am-241 = 2.1/54.5/25.0/9.3/6.4/2.7 %.

3.2. 3×3 multicell problems including burnable absorber

Two 3×3 multicell problems were prepared. In both the problems, one Gd-bearing UO_2 rod is surrounded by normal UO_2 fuel rods. The Gd content and the uranium-235 enrichment of the center rod are 10 wt% and 4.0 wt%, respectively. The geometrical specification and the composition of the peripheral normal UO_2 fuel in the first problem was taken from the single pincell problems in the preceding subsection. The uranium-235 enrichment is 4.1 wt%. The second problem is based on the PWR-UO_2 assembly prepared by the working party on reactor physics for LWR next generation fuels of the research committee of reactor physics in Japan Atomic Energy Research Institute[23]. Uranium-235 enrichment of the normal UO_2 rod is 6.5 wt%. The brief geometrical specification of these problems is shown in **Figure 1**.

[Figure 1 about here.]

3.3. PWR fuel assembly problems

Two PWR fuel assembly problems were taken from the VERA benchmark problem[24], and these are denoted to as VERA-2O and -2P. The UO_2 fuel rods contain the fuel of the 3.1 wt% uranium-235 enrichment while the Gd-bearing rods contain 1.8 wt% uranium-235 and 5 wt% Gd_2O_3 in both the problems. The numbers of the loaded Gd-bearing rods are 12 for VERA-2O and 24 for VERA-2P. The brief geometrical specifications are shown in Figure 1.

4. Numerical results

4.1. Single pincell problems

The infinite neutron multiplication factors during fuel depletion of the four single pincell problems calculated with JENDL-4.0 are shown in **Fig. 2** and the relative differences in k_∞ from the reference JENDL-4.0 results are shown in **Fig. 3** for JENDL-5, ENDF/B-VIII.0, and JEFF-3.3. The trend between the UO_2 and MOX fuels is different, while the differences among the UO_2 fuels with the different enrichments are insignificant. In the following, the UO_2 fuel only with the enrichment of 4.1 wt% is concerned.

[Figure 2 about here.]

[Figure 3 about here.]

Figure 4 shows relative differences in k_∞ from the reference for the UO_2 and MOX single pincell problems. The data points shown on these figures are relative differences directly calculated from the values of k_∞, and the lines are those estimated from the sensitivity coefficients and the differences in the cross sections. Generally good agreement is obtained between them. The differences between them might be caused by several possibilities including the first-order approximation in the sensitivity analyses, the limitation in the nuclear data considered in the indirect component, and the inconsistency of the multi-group cross sections in Eq. (5).

At the beginning of the depletion of the UO_2 pincell problem, differences in k_∞ among the different nuclear data files are less than approximately 0.4%, but those become large with the fuel burnup increases. Relatively low estimation of k_∞ by ENDF/B-VIII.1, ENDF/B-VIII.0, JEFF-3.2, JENDL-5, and JEFF-3.3 compared with the reference becomes large with the fuel burnup, and the low estimation of JEFF-3.3 reaches over 1.0 % at 45 GWD/t. Only the result by ENDF/B-VII.1 shows similar trend with the reference JENDL-4.0 result. **Figure 5** shows nuclear data-wise relative differences in k_∞ of the single UO_2 pincell problem from the reference.

- The low k_∞ values with depletion compared with the reference would come from several nuclear data such as (n,f), (n,γ), and $\bar{\nu}$ of Pu-239, and (n,γ) of U-238. The significantly low k_∞ value with depletion observed in the JEFF-3.3 result comes from (n,γ) and $\bar{\nu}$ of Pu-239 and (n,γ) of U-238.
- The k difference coming from oxygen absorption cross sections is caused by the difference above several MeV, so this may come from the difference in the (n,α) reaction.
- On the differences of JENDL-5, ENDF/B-VIII.0, and ENDF/B-VIII.1 from the reference, contributions of U-235 are cancelled out among (n,f), (n,γ), and $\bar{\nu}$. **Figure 6** shows energy-group break down in the sensitivity analyses results of JENDL-5. Mainly the thermal energy range below 0.1 eV is dominant, but the (n,γ) contribution is relatively large in the range from 0.1 eV to 1 eV compared with the (n,f) contribution.

The comparison between the results of ENDF/B-VIII.0 and ENDF/B-VIII.1 would be interesting since ENDF/B-VIII.0 tends to underestimate the reactivity of pressurized water reactors during the fuel depletion compared with the old file, ENDF/B-VII.1[4]. When comparing the ENDF/B-VIII.0 result with the ENDF/B-VIII.1 result, the revision in (n,f) of Pu-239 and (n,γ) of U-238 would contribute to moderate the low k_∞ value

during depletion.

On the MOX pincell problem, large differences in k_∞ are observed at the beginning of the fuel depletion, but the burnup dependence of the k_∞ difference is not significant as the UO_2 pincell problem as shown in Fig. 4. In the results of ENDF/B-VIII.0 and JEFF-3.3, relatively large dependences on the fuel burnup are observed. **Figure 7** shows nuclear data-wise relative differences in k_∞ of the single MOX pincell problem from the reference. It is interesting to point out that the difference in the H-1 thermal scattering data has large impact, and all the concerned nuclear data files show similar trend with each other. Also, the differences in (n,γ) of Am-241 have large impact and shows the significant burnup dependence in the results of JENDL-5, JEFF-3.2, and -3.3. Since the resonance parameters of Am-241 in ENDF/B-VII.1, -VIII.0, and -VIII.1 are taken from those in JENDL-4.0, no significant differences caused by Am-241 (n,γ) are not observed in the results of these files. In the revision from ENDF/B-VIII.0 to ENDF/B-VIII.1, $\bar{\nu}$ of Pu-239 and (n,γ) of Pu-240 have relatively large impacts on k_∞.

[Figure 4 about here.]

[Figure 5 about here.]

[Figure 6 about here.]

[Figure 7 about here.]

4.2. 3×3 multicell problems including burnable absorber

Figure 8 shows k_∞ of the 3×3 multicell problem with the 4.1 wt% UO_2 fuel and the relative difference from the reference JENDL-4.0 result. Around the beginning of the fuel depletion, the differences in k_∞ show similar behavior to those in the UO_2 single pincell problem. Until the Gd burnout around 20 GWD/t, the difference in k_∞ from the reference tends to shift to the positive side compared with the single UO_2 pincell problem except JENDL-5. In the JENDL-5 result, decrease in the k_∞ difference from the reference becomes

more significant until the Gd burnout, and after the Gd burnout it slightly increases for the next 5 GWD/t and begins to decrease. **Figure 9** shows the nuclear data-wise relative differences in k_∞ from the reference. Around the beginning of the depletion, the difference in (n,γ) of Gd-157 causes low k_∞ values over 0.2% compared with the reference and this is common for all the concerned nuclear data files. This suggests that Gd-157 (n,γ) cross sections of JENDL-4.0 are larger than those of the other nuclear data files, and Gd-157 burns out more quickly during the fuel depletion. Also the difference in the thermal scattering cross sections of H-1 causes large k_∞ values with the depletion until the Gd burnout in all these results. Mainly due to the above two mechanism, the k_∞ difference from the reference shows different trend from that in the UO_2 single pincell problem until the Gd burnout. In the JENDL-5 result, the difference in (n,γ) of Gd-155 cancels the effect of (n,γ) of Gd-157 out. This result suggests that (n,γ) of Gd-155 in the JENDL-5 evaluation is different from that of all the other files.

[Figure 8 about here.]

[Figure 9 about here.]

Figure 10 shows k_∞ of the 3×3 multicell problem with the 6.5 wt% UO_2 fuel and the relative difference from the reference JENDL-4.0 result. Whereas the burnup point of the Gd burnout is different from that in the first 3×3 multicell problem, the trends of the k_∞ differences from the reference are very similar. **Figure 11** shows the nuclear data-wise relative differences in k_∞ from the reference. When comparing with the preceding result, the impact of the difference in (n,f) of U-235 is slightly moderated and that in (n,γ) of U-235 is enhanced due to the relatively large value of the uranium enrichment and the neutron flux energy spectrum hardening. This can be understood from the energy group break down information shown in Figure 6.

[Figure 10 about here.]

[Figure 11 about here.]

4.3. PWR fuel assembly model

Figures 12 and **13** show k_∞ and the relative difference from the reference JENDL-4.0 results for VERA-2O and VERA-2P, respectively. The trends before the Gd burnout are very similar with those of the 3×3 multicell problem and those after the Gd burnout are very similar with those of the UO_2 single pincell problem. Thus, the detailed nuclear data-wise sensitivity analysis result is omitted here.

[Figure 12 about here.]

[Figure 13 about here.]

5. Conclusion

Burnup calculations were carried out for the LWR single pincell problems, the 3×3 multicell problems, and the PWR assembly problems with the modern evaluated nuclear data files, and the differences in the neutron multiplication factors from the reference JENDL-4.0 results were obtained. Furthermore, the origin of these k differences was investigated through the sensitivity analyses using the sensitivity coefficients and the cross section differences. The sensitivity analysis results show that the UO_2 single pincell problem with different enrichment, 3.4 wt%, 4.1 wt% and 4.7 wt%, do not give any significant differences in the k_∞ trend, while comparing the UO_2 and MOX fuels give the significant differences. Regarding the 3×3 multicell problems with the burnable absorbers changes the k_∞ trend compared with those of the single cell problems due to the contributions from Gd-155 and -157 (n,γ) cross sections and the H-1 thermal scattering cross sections. The PWR assembly problems show the similar trend in the k_∞ differences with those of the 3×3 multicell problems and the single pincell problems.

Acknowledgement

Hidayati Amar was a fellow of the Nuclear Researchers Exchange Programme 2024 supported by the Ministry of Education, Culture, Sports, Science, and Technology and the Nuclear Safety Research Association of Japan.

References

[1] Plompen AJM, Cabellos O, De Saint Jean C, et al. The joint evaluated fission and fusion nuclear data library, JEFF-3.3. European. Phys. Journal A. 2020; 56:181_1.

[2] Iwamoto O, Iwamoto N, Kunieda S, et al. Japanese evaluated nuclear data library version 5: JENDL-5. J Nucl Sci Technol. 2023; 60:1-60.

[3] Brown D, Chadwick M, Capote R, et al. ENDF/B-VIII.0: the 8th major release of the nuclear reaction data library with CIELO-project cross sections, new standards, and thermal scattering data. Nucl Data Sheets. 2018; 148:1-142.

[4] Kim KS, Wieselquist WA. Reactivity underestimation of ENDF/B-VIII.0 compared with ENDF/B-VII.1 for the pressurized water reactor depletion analysis. Trans Am Nucl Soc. 2021; 124:520-523.

[5] Ohki S, Jin T. Dependence of fast reactor fuel burnup characteristics opn nuclear data libraries. J Nucl Sci Technol. 2005; 42:390-397.

[6] Stauff NE, Aliberti G, Kim TK, Taiwo TA. Impact of the differences in nuclear data on estimated k-effective of SFR cores. Proc. Int. Conf. on Reactor Physics; 2014 Sep 28-Oct 3; Kyoto, Japan.

[7] Kawamoto Y, Chiba G, Tsuji M, et al. Nuclear data sensitivity analysis for isotopic generation using JENDL-4.0, ENDF/B-VII.1 and JEFF-3.1.1. Proc. Int. Conf. on Reactor Physics; 2014 Sep 28-Oct 3; Kyoto, Japan.

[8] Gandini A. A method of correlation of burnup measurements for physics prediction of fast power-reactor life. Nucl Sci Eng. 1969; 38: 1-7.

[9] Williams ML. Development of depletion perturbation theory for coupled neutron/nuclide fields. Nucl Sci Eng. 1979; 70: 20-36.

[10] Chiba G, Harada H. Validation of LWR fuel depletion calculation module of reactor physics code system CBZ. J Nucl Sci Technol. 2023; 60:969-979.

[11] Shibata K, Iwamoto O, Nakagawa T, et al. JENDL-4.0: A new library for nuclear science and technology. J Nucl Sci Technol. 2011; 48:1-30.

[12] Hebert A, Santamarina A. Refinement of the Santamarina-Hfaiedh energy mesh between 22.5 eV and 11.4 keV. Proc. Int. Conf. on Reactor Physics; 2008 Sep 14-19; Interlaken, Switzerland.

[13] Tada K, Yamamoto A, Kunieda S, et al. Development and verification of nuclear data processing code FRENDY version 2. J Nucl Sci Technol. 2024; 61:830-839.

[14] MacFarlane RE, Kahler AC. Methods for processing ENDF/B-VII with NJOY. Nucl Data Sheets. 2010; 111: 2739-2890.

[15] Chiba G, Narabayashi T. Advanced Bondarenko method for resonance self-shielding calculations in deterministic reactor physics code system CBZ. Ann Nucl Energy. 2016; 96:277-286.

[16] Sugimura N, Yamamoto A. Evaluation of Dancoff factors in complicated geometry using the method of characteristics. J Nucl Sci Technol. 2006; 43:1182-1187.

[17] Kawamoto Y, Chiba G, Tsuji M, et al. Numerical solution of matrix exponential in burn-up equation using mini-max polynomial approximation. J Nucl Sci Technol. 2015; 80:219-224.

[18] Chiba G, Ohoka Y, Yamamoto K, et al. Revisiting mini-max polynomial approximation method for nuclear fuel depletion calculations. Proc. Int. Conf. on Math. Comp. Methods Applied to Nucl. Sci. Eng.; 2019 Aug 25-29; Portland (OR).

[19] Sasuga J, Chiba G, Ohoka Y, Yamamoto K, Kodama Y, Nagano H. Improvement of the optimally-weighted predictor-corrector method for nuclear fuel burnup calculations. J Nucl Sci Technol. 2021; 58:1134-1144.

[20] Chiba G, Tsuji M, Narabayashi T, Ohoka Y, Ushio T. Important fission product nuclides identification method for simplified burnup chain construction. J Nucl Sci Technol. 2015; 52:953-960.

[21] Katakura J. JENDL FP decay data file 2011 and fission yields data file 2011. Japan: Japan Atomic Energy Agency; 2011, JAEA-Data/Code 2011-025.

[22] Okumura K, Kugo T, Kaneko K, Tsuchihashi K. SRAC2006: a comprehensive neutronics calculation code system. Japan: Japan Atomic Energy Agency; 2007, JAEA-Data/Code 2007-004.

[23] Yamamoto A, Ikehara T, Ito T, et al. Benchmark problem suite of reactor physics study of LWR next generation fuels. J Nucl Sci Technol. 2002; 39:900-912.

[24] Kim KS. Specification for the VERA depletion benchmark suite, Oak Ridge National Laboratory; 2015, CASL-U-2015-PHI-.CVS.P11, 02-010.

Figure Captions

Figure 1 Geometrical specifications of the 3×3 multicell problems (left) and the PWR fuel assembly problems (center and right)

Figure 2 k_∞ of the single pincell problems obtained with JENDL-4.0

Figure 3 Relative differences in k_∞ of the single pincell problems using the JENDL-4.0 results as the reference

Figure 4 Relative differences in k_∞ of the single pincell problems using the JENDL-4.0 results as the references

Figure 5 Nuclear data-wise relative differences in k_∞ of the single UO_2 pincell problem using the JENDL-4.0 result as the reference

Figure 6 Energy-group break-down in the sensitivity analysis results of JENDL-5 of the single UO_2 pincell problem

Figure 7 Nuclear data-wise relative differences in k_∞ of the single MOX pincell problem using the JENDL-4.0 result as the reference

Figure 8 k_∞ of the 3×3 multicell problem with the 4.1 wt% UO_2 fuel (left) and the relative difference from the reference JENDL-4.0 result (right)

Figure 9 Nuclear data-wise relative difference in k_∞ of the 3×3 multicell problem with the 4.1 wt% UO_2 fuel

Figure 10 k_∞ of the 3×3 multicell problem with the 6.5 wt% UO_2 fuel (left) and

the relative difference from the reference JENDL-4.0 result (right)

Figure 11 Nuclear data-wise relative difference in k_∞ of the 3×3 multicell problem with the 6.5 wt% UO_2 fuel

Figure 12 k_∞ of VERA-2O (left) and the relative difference from the reference JENDL-4.0 result (right)

Figure 13 k_∞ of VERA-2P (left) and the relative difference from the reference JENDL-4.0 result (right)

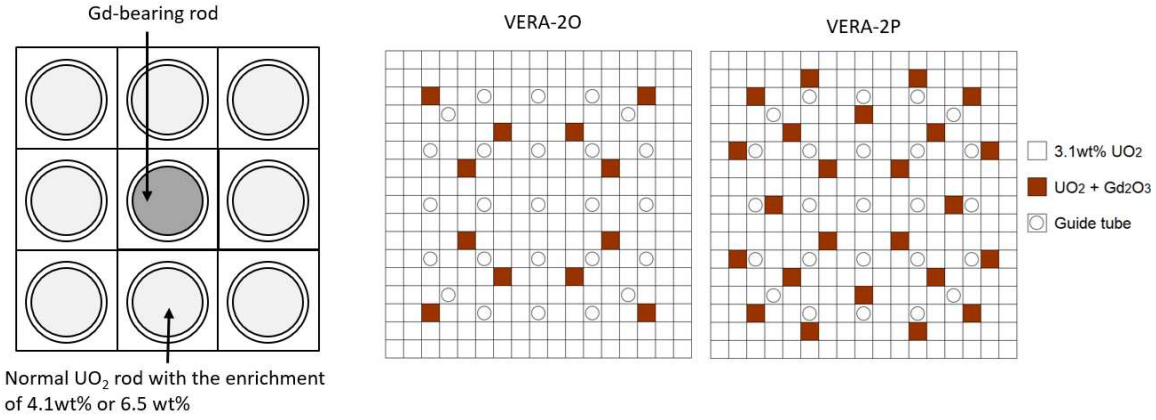

Figure 1 Geometrical specifications of the 3×3 multicell problems (left) and the PWR fuel assembly problems (center and right)

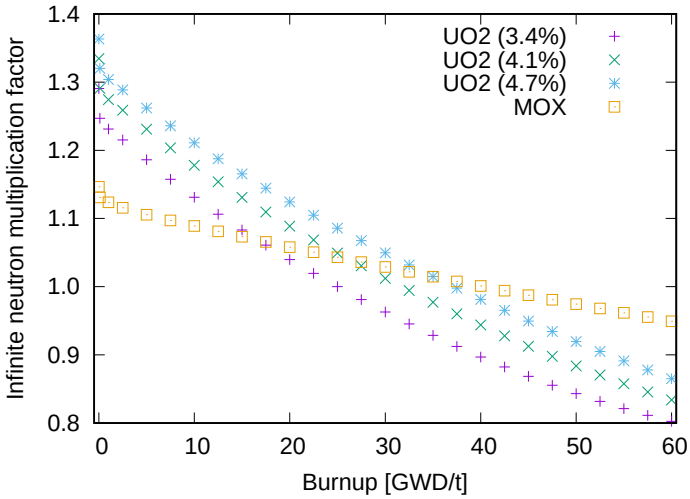

Figure 2 k_∞ of the single pincell problems obtained with JENDL-4.0

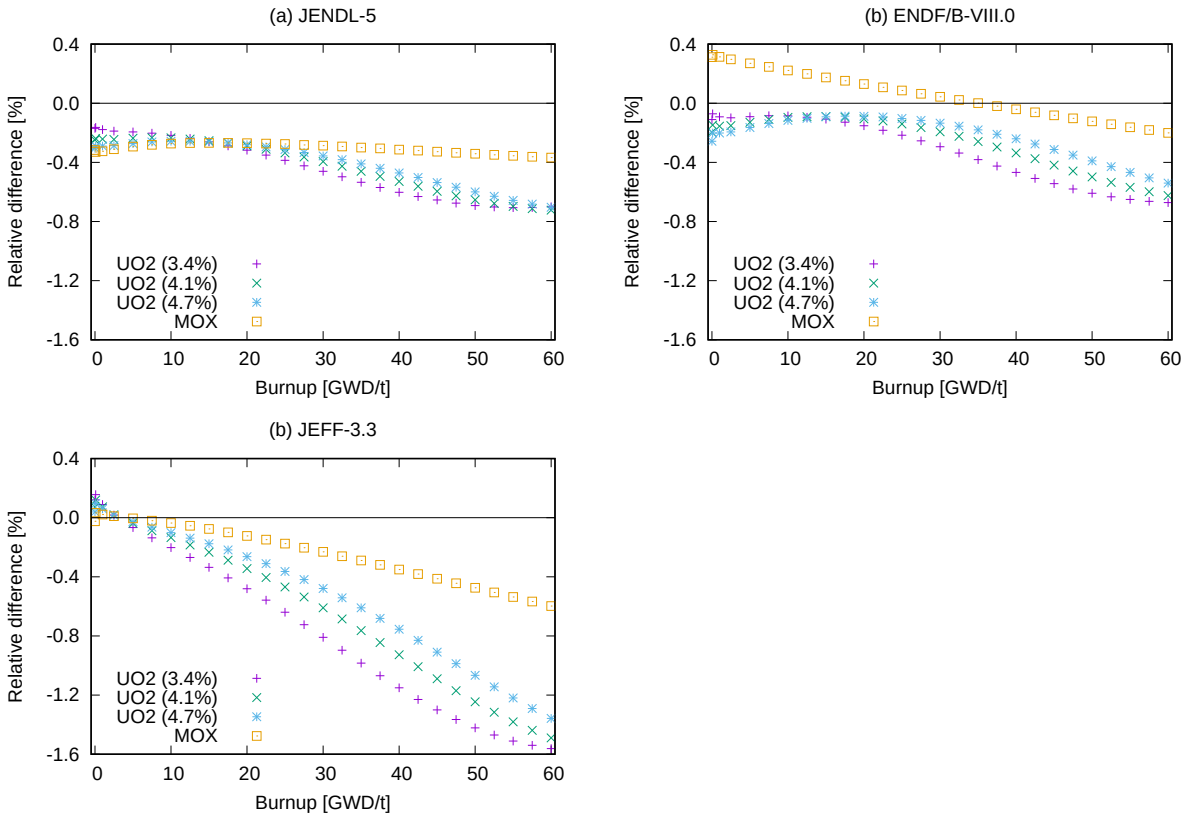

Figure 3 Relative differences in k_∞ of the single pincell problems using the JENDL-4.0 results as the reference

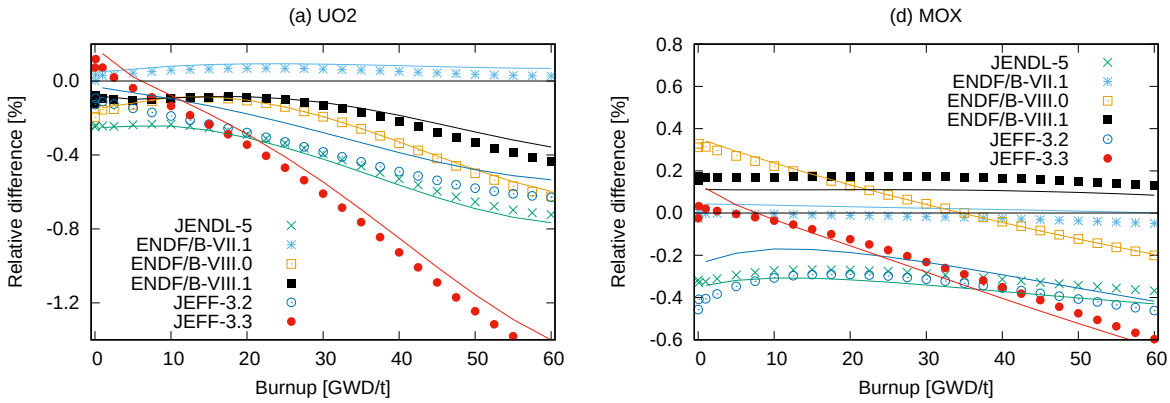

Figure 4 Relative differences in k_∞ of the single pincell problems using the JENDL-4.0 results as the references

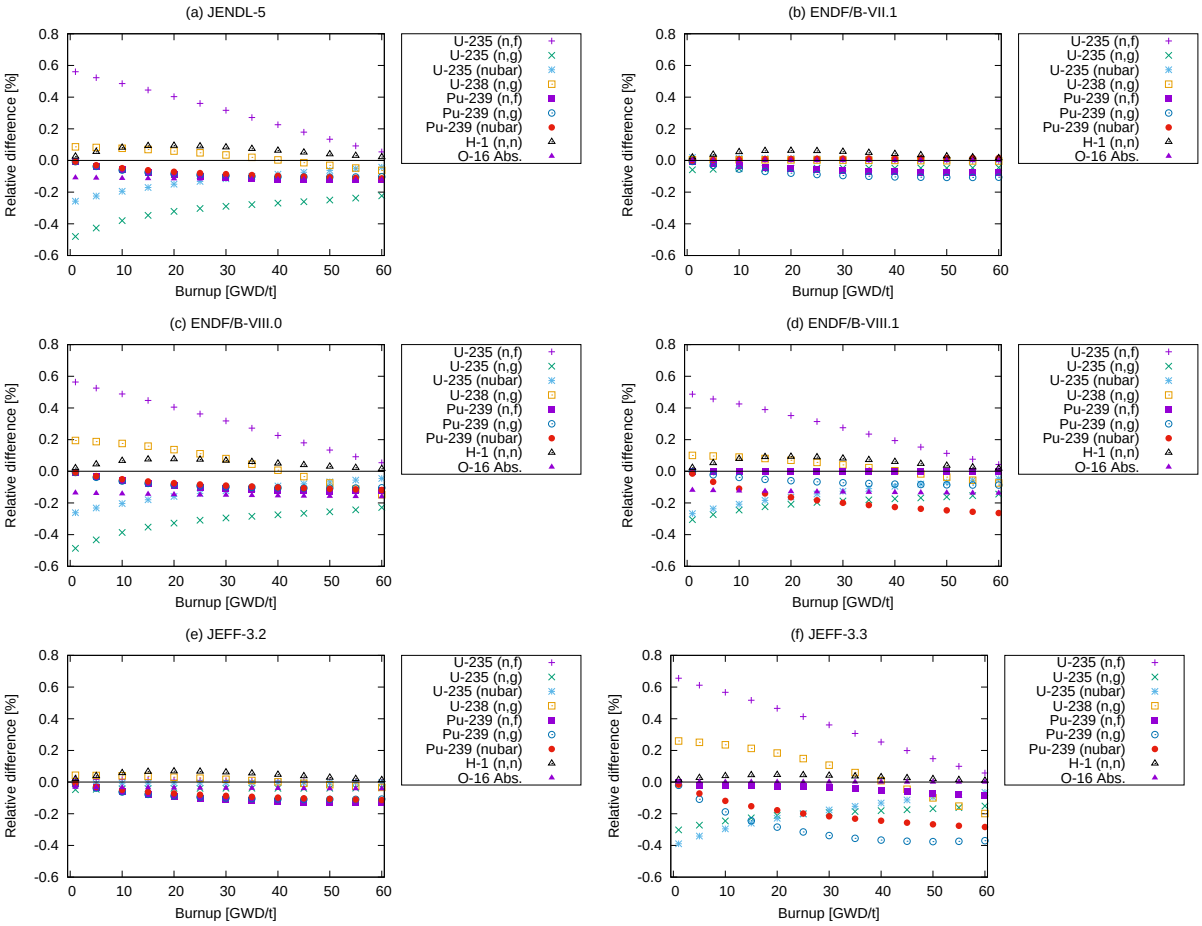

Figure 5 Nuclear data-wise relative differences in k_∞ of the single UO_2 pincell problem using the JENDL-4.0 result as the reference

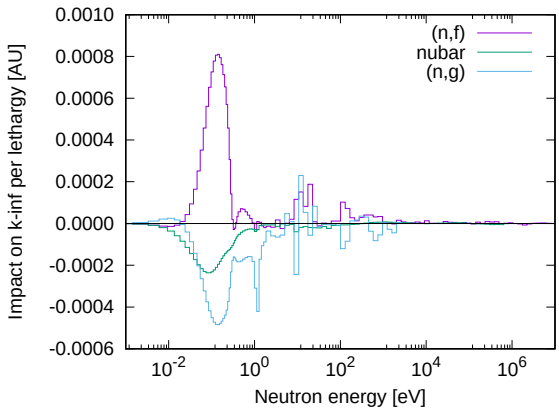

Figure 6 Energy-group break-down in the sensitivity analysis results of JENDL-5 of the single UO_2 pincell problem

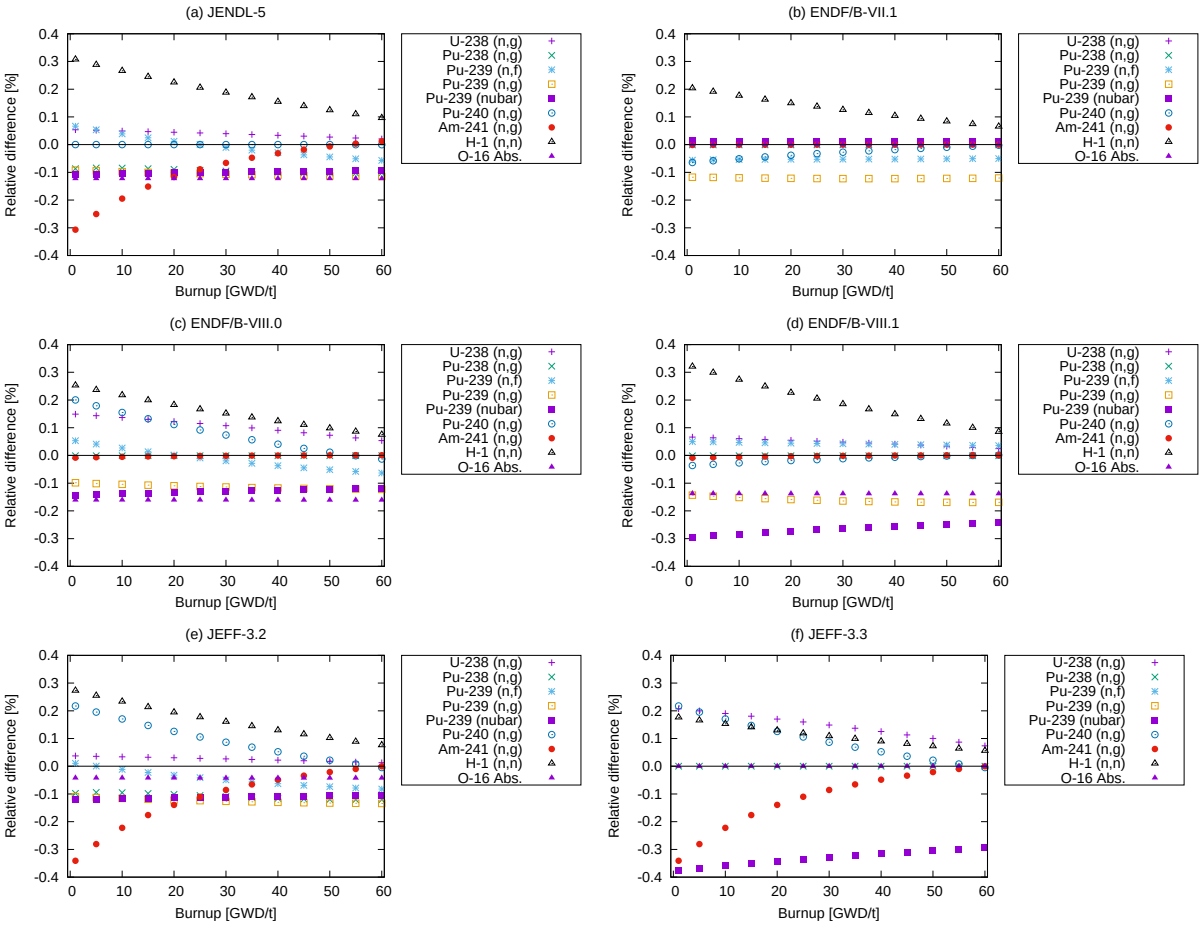

Figure 7 Nuclear data-wise relative differences in k_∞ of the single MOX pincell problem using the JENDL-4.0 result as the reference

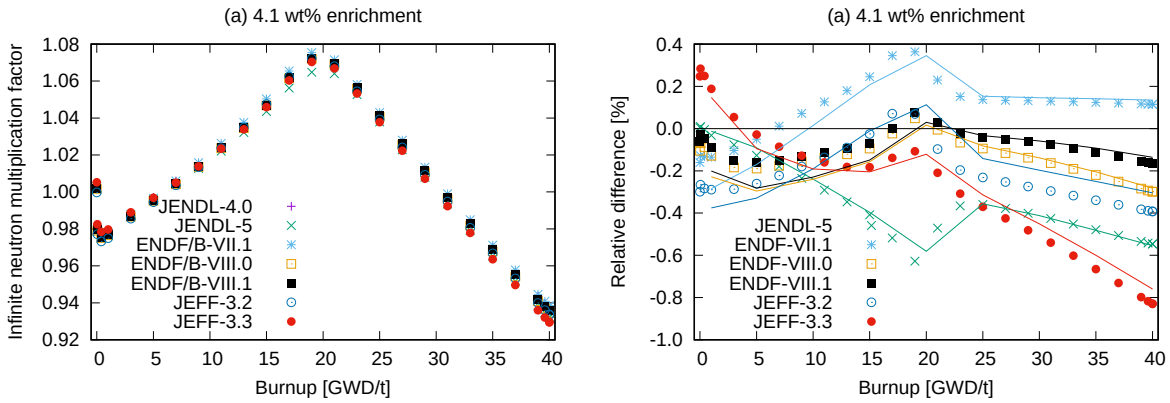

Figure 8 k_∞ of the 3×3 multicell problem with the 4.1 wt% UO_2 fuel (left) and the relative difference from the reference JENDL-4.0 result (right)

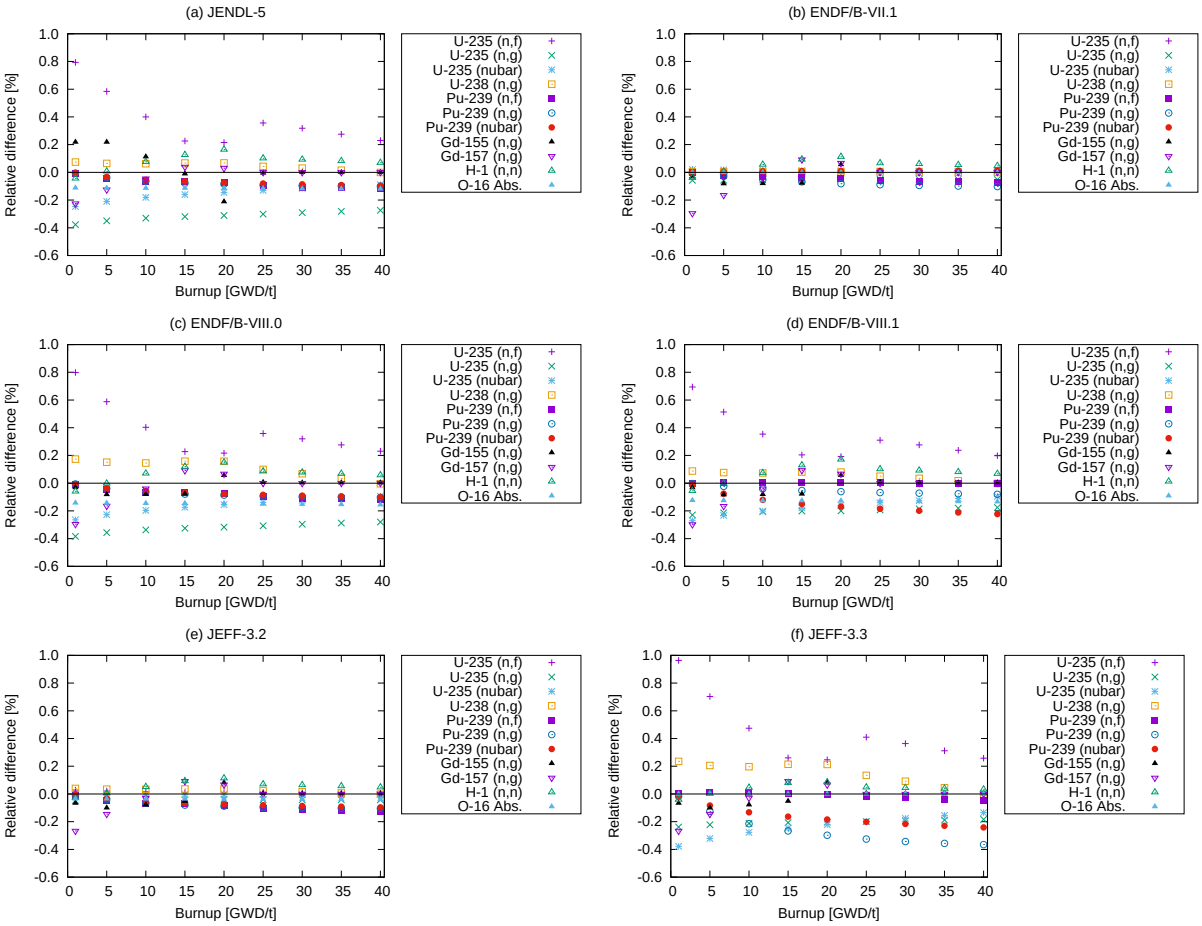

Figure 9 Nuclear data-wise relative difference in k_∞ of the 3×3 multicell problem with the 4.1 wt% UO_2 fuel

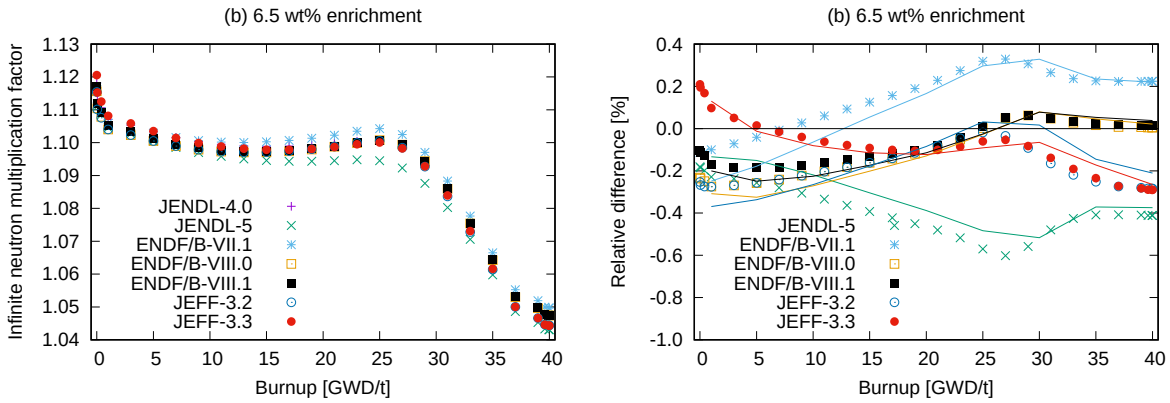

Figure 10 k_∞ of the 3×3 multicell problem with the 6.5 wt% UO_2 fuel (left) and the relative difference from the reference JENDL-4.0 result (right)

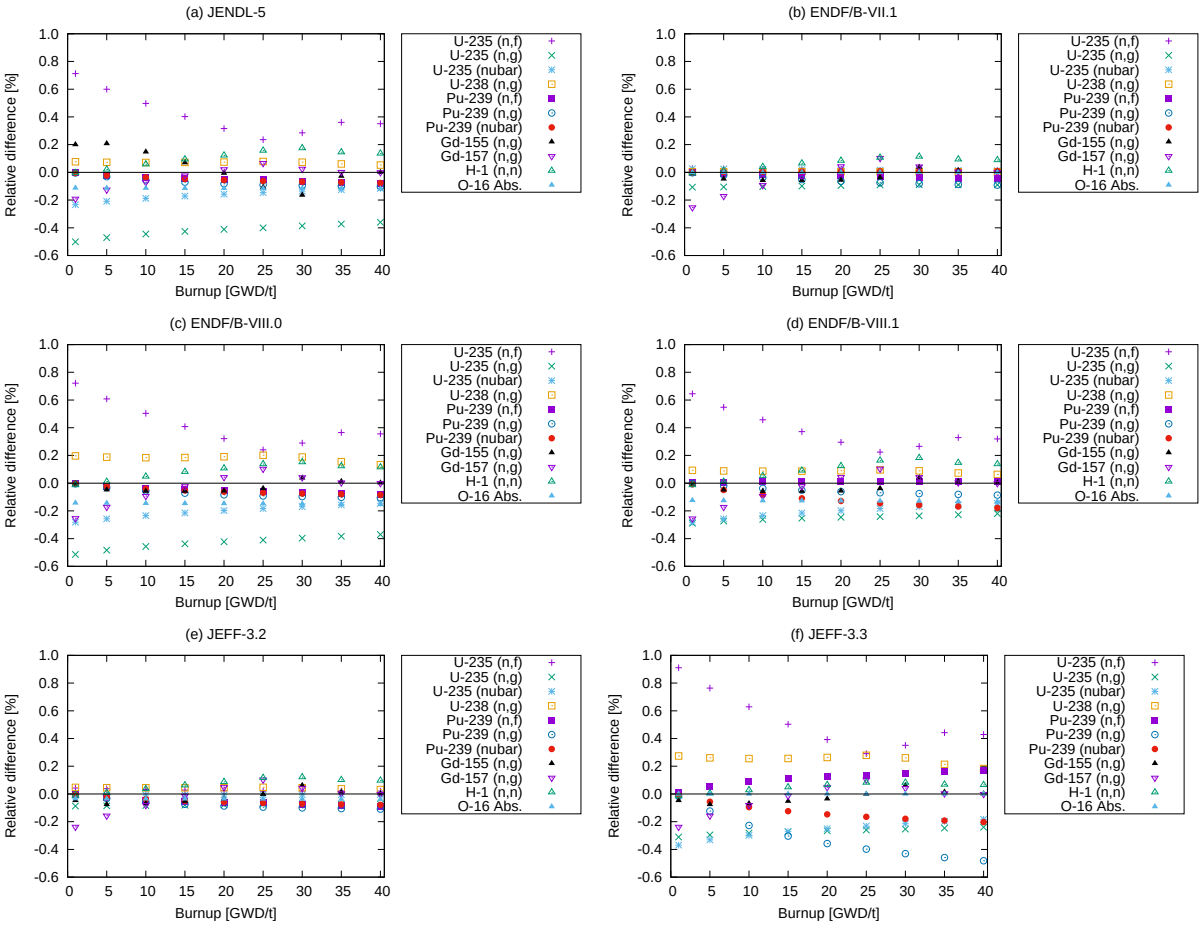

Figure 11 Nuclear data-wise relative difference in k_∞ of the 3×3 multicell problem with the 6.5 wt% UO_2 fuel

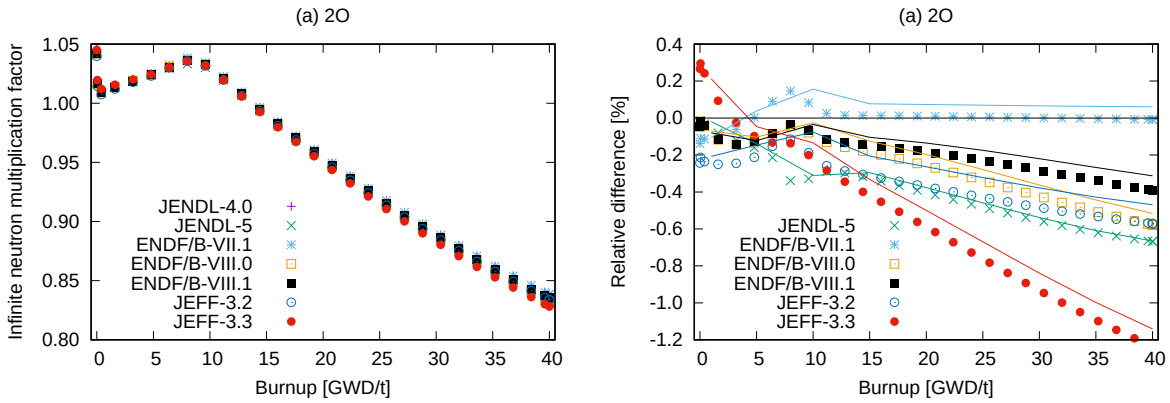

Figure 12 k_∞ of VERA-2O (left) and the relative difference from the reference JENDL-4.0 result (right)

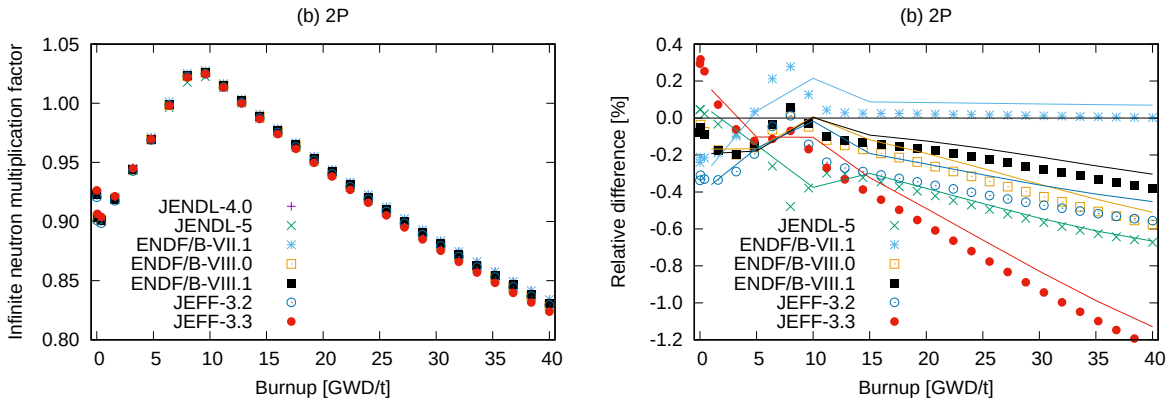

Figure 13 k_∞ of VERA-2P (left) and the relative difference from the reference JENDL-4.0 result (right)